SIAM J. SCI. COMPUT.
Vol. 31, No. 4, pp. 2528–2548

A LOCALLY CONSERVATIVE FINITE ELEMENT METHOD BASED ON PIECEWISE CONSTANT ENRICHMENT OF THE CONTINUOUS GALERKIN METHOD*

SHUYU SUN† AND JIANGGUO LIU‡

Abstract. This paper presents a locally conservative finite element method based on enriching the approximation space of the continuous Galerkin method with elementwise constant functions. The proposed method has a smaller number of degrees of freedom than the discontinuous Galerkin method. Numerical examples on coupled flow and transport in porous media are provided to illustrate the advantages of this method. We also present a theoretical analysis of the method and establish optimal convergence of numerical solutions.

Key words. continuous Galerkin methods, discontinuous Galerkin methods, enriched Galerkin methods, flow, locally conservative methods, transport

AMS subject classifications. 65M60, 65N30, 76S05

DOI. 10.1137/080722953

1. Introduction.

The standard continuous Galerkin (CG) finite element method is widely used for solving second-order elliptic problems due to its simple implementation compared with the mixed finite element (MFE) and the discontinuous Galerkin (DG) methods. However, CG suffers from its inability to provide locally conservative flux approximations, which is a much needed property in many applications, especially when streamlines are to be constructed or when flow is coupled with transport. In the latter, violation of local conservation in velocity fields could cause spurious sources and sinks to transport simulations, which might lead to substantial numerical inaccuracy of transport solutions, including overshoots and undershoots. Those concentration overshoots and undershoots could be even worsened if reaction is also presented in the system. With the goal to preserve this important property of conservation, many locally conservative methods have been developed in the literature, which include primal DG methods, continuous and discontinuous MFE methods, control volume MFE methods, finite volume element methods, mimetic finite difference methods, and multipoint flux approximation methods. In addition to this, quite a few efforts have also been focused on the recovery of local mass conservation for nonconservative schemes, especially for CG [10, 11, 16, 19, 30].

Being locally conservative by design, the DG methods [2, 5, 6, 9, 12, 15, 17, 18, 20, 21, 22, 23, 26, 27, 29, 31, 32, 33] are specialized finite element methods that utilize discontinuous piecewise polynomial spaces to approximate the solutions of differential equations, with interelement continuity and boundary conditions weakly imposed through bilinear forms. The local conservation of DG is a result of its derivation from variational principles by integration over local cells. Weak enforcement of boundary conditions and interelement continuity leads to small numerical diffusion and little

*Received by the editors April 30, 2008; accepted for publication (in revised form) March 31, 2009; published electronically June 12, 2009.
http://www.siam.org/journals/sisc/31-4/72295.html
†Department of Mathematical Sciences, Clemson University, Clemson, SC 29634-0975 (shuyu@clemson.edu).
‡Department of Mathematics, Colorado State University, Fort Collins, CO 80523-1874 (liu@math.colostate.edu).

oscillation in numerical solutions. In addition, the DG methods handle rough coefficient problems and capture the discontinuity in solutions very well due to the nature of discontinuous function spaces. Examples of the DG methods include local discontinuous Galerkin (LDG) [12, 13], symmetric interior penalty Galerkin (SIPG) [25, 28, 33], Oden–Babuška–Baumann-DG (OBB-DG) formulation [20], nonsymmetric interior penalty Galerkin (NIPG) [22], and incomplete interior penalty Galerkin (IIPG) methods [14, 25, 28]. One major disadvantage of the DG methods is that they have much larger numbers of unknowns than the CG methods.

In this paper, we present a locally conservative finite element method based on enriching the approximation space of the CG method with elementwise constant functions. The proposed enriched Galerkin (EG) method uses a weak formulation similar to that of DG, but it has a smaller number of degrees of freedom than DG.

We comment that the EG method proposed in this paper is different from the postprocessing procedures discussed in [10, 11, 19, 30]. For example, the postprocessing methods in [30] consist of correcting existing normal fluxes (obtained from other methods) on element boundaries and then extending correction into element interiors. The postprocessing in [19] is also based on computing a correction of the average normal flux on an edge or face. The correction is a jump in a piecewise constant or linear function. This approach is also in line with the two-step postprocessing discussed in [11]. The first step there is the computation of a numerical flux trace defined on edges or faces. This computation is nonlocal, but the system to be solved is well-conditioned. The second step in [11] is a local element-by-element postprocessing based on the Raviart–Thomas projection. This leads to a conservative flux approximation with continuous normal components. In contrast to those postprocessing approaches, we incorporate the enrichment of a proper approximation subspace into the weak formulation of EG. Local mass conservation is attained in the numerical solutions of EG directly. Therefore, we comment that EG should be a viable alternative to the mixed method, DG, or CG postprocessing. In the preprint [8], Becker et al. have also considered a linear (P1) CG space enriched with piecewise constant functions and applied it to time-independent convection-diffusion and Stokes problems. This paper differs from [8] in its emphasis on the coupled flow and transport simulations. Here, we illustrate a simple technique for solving the flow equation and for constructing a conservative flux for use in subsequent transport simulations. Our piecewise constant enrichment applies to high-order CG spaces as well.

The paper is organized as follows. In section 2, we state the modeling equations of flow and transport in porous media and review the classical CG and DG methods for the model problems. Then we propose the EG method based on enrichment of the finite element space in the CG formulation. An analysis of the EG method is carried out in section 3. Section 4 presents numerical experiments to illustrate the advantages of the new method. These include examples of highly varied and randomly varied permeability/conductivity fields, with linear and higher-order approximations on rectangular and triangular grids. In section 5, we first summarize and discuss various behaviors and features of EG and then conclude this paper with possible future work.

2. Governing equations and numerical schemes.

2.1. Governing equations.

We consider coupled flow and reactive transport within a single flowing phase in porous media. The velocity computed from the flow equation will be used for simulations of the concentration in the transport equation. Local mass conservation of the velocity is crucial in this application.

For convenience, we assume Ω is a bounded polygonal domain in $\mathbb{R}^d$ ($d = 1$, 2, or 3) with boundary $\partial\Omega$, and the flow equation has the following form:

$$-\nabla \cdot (\mathbf{K}\nabla p) \equiv \nabla \cdot \mathbf{u} = q, \qquad (x,t) \in \Omega \times (0,T]. \tag{2.1}$$

The unknowns are the pressure p and the Darcy velocity $\mathbf{u}$. We assume that the conductivity $\mathbf{K}$ (the ratio of the permeability and the viscosity) is uniformly symmetric positive definite and bounded from above and below. We impose a Dirichlet boundary condition for the flow equation on Γ_{D} and a Neumann boundary condition on Γ_{N} ($\overline{\Gamma}_{\mathrm{D}} \cup \overline{\Gamma}_{\mathrm{N}} = \partial\Omega$, $\Gamma_{\mathrm{D}} \cap \Gamma_{\mathrm{N}} = \emptyset$):

$$\mathbf{u} \cdot \mathbf{n} \equiv -\mathbf{K}\nabla p \cdot \mathbf{n} = u_B, \qquad x \in \Gamma_{\mathrm{N}}, \tag{2.2}$$

$$p = p_B, \qquad x \in \Gamma_{\mathrm{D}}, \tag{2.3}$$

where $\mathbf{n}$ denotes the unit outward normal vector on $\partial\Omega$.

The classical equation of reactive transport in porous media is

$$\frac{\partial \phi c}{\partial t} + \nabla \cdot (\mathbf{u}c - \mathbf{D}\nabla c) = qc^* + r(c), \qquad (x,t) \in \Omega \times (0,T], \tag{2.4}$$

equipped with the boundary conditions

$$(\mathbf{u}c - \mathbf{D}\nabla c) \cdot \mathbf{n} = c_B \mathbf{u} \cdot \mathbf{n}, \qquad (x,t) \in \Gamma_{\mathrm{in}} \times (0,T], \tag{2.5}$$

$$(-\mathbf{D}\nabla c) \cdot \mathbf{n} = 0, \qquad (x,t) \in \Gamma_{\mathrm{out}} \times (0,T]. \tag{2.6}$$

Here T is the final simulation time; c_B denotes the inflow concentration; $\partial\Omega = \overline{\Gamma}_{\mathrm{in}} \cup \overline{\Gamma}_{\mathrm{out}}$ with $\Gamma_{\mathrm{in}} := \{x \in \partial\Omega : \ \mathbf{u} \cdot \mathbf{n} < 0\}$ the inflow boundary and $\Gamma_{\mathrm{out}} := \{x \in \partial\Omega : \mathbf{u} \cdot \mathbf{n} \geq 0\}$ the outflow/no-flow boundary. The diffusion-dispersion tensor $\mathbf{D}$ can be a function of $\mathbf{u}$, but we primarily focus on the advection component of transport in this paper. An initial concentration is specified to close the system

$$c(x,0) = c_0(x), \qquad x \in \Omega. \tag{2.7}$$

2.2. Notation. Let $\mathcal{E}_h$ be a family of nondegenerate quasi-uniform and possibly nonconforming partitions of Ω composed of line segments if $d = 1$, triangles or quadrilaterals if $d = 2$, or tetrahedra, prisms, or hexahedra if $d = 3$. The nondegeneracy requirement (also called regularity) is that the element is convex, and that there exists $\rho > 0$ such that if h_j is the diameter of $E_j \in \mathcal{E}_h$, then each of the subtriangles (for $d = 2$) or subtetrahedra (for $d = 3$) of element E_j contains a ball of radius ρh_j in its interior. The quasi-uniformity requirement is that there exists $\tau > 0$ such that $h \leq \tau h_j$ for all $E \in \mathcal{E}_h$, where h is the maximum diameter of all elements. We assume that the mesh is aligned with the interfaces between Γ_{D} and Γ_{N} and the interfaces between Γ_{in} and Γ_{out}. The set of all interior faces (for $d = 3$; "faces" meaning edges for $d = 2$ or nodes for $d = 1$) for $\mathcal{E}_h$ is denoted by Γ_h. On each face $\gamma \in \Gamma_h$, a unit normal vector $\mathbf{n}_\gamma$ is chosen. The set of all faces on Γ_{D}, Γ_{N}, Γ_{in}, and Γ_{out} for $\mathcal{E}_h$ is denoted by $\Gamma_{h,\mathrm{D}}$, $\Gamma_{h,\mathrm{N}}$, $\Gamma_{h,\mathrm{in}}$, and $\Gamma_{h,\mathrm{out}}$, respectively, for which the normal vector $\mathbf{n}_\gamma$ coincides with the outward unit normal vector.

For $s \geq 0$, we define

$$H^s(\mathcal{E}_h) := \left\{\phi \in L^2(\Omega) : \ \phi|_E \in H^s(E), \ E \in \mathcal{E}_h\right\}. \tag{2.8}$$

We now define the average and jump for $\phi \in H^s(\mathcal{E}_h)$, $s > 1/2$. Let $E_i, E_j \in \mathcal{E}_h$ and $\gamma = \partial E_i \cap \partial E_j \in \Gamma_h$ with $\mathbf{n}_\gamma$ exterior to E_i. Denote

$$\{\phi\} := \frac{1}{2}\Big((\phi|_{E_i}) \Big|_\gamma + \big(\phi|_{E_j}\big) \Big|_\gamma \Big), \tag{2.9}$$

$$[\phi] := (\phi|_{E_i}) \Big|_\gamma - \big(\phi|_{E_j}\big) \Big|_\gamma. \tag{2.10}$$

Denote the upwind value of concentration $c^*|_\gamma$ as follows:

$$c^*|_\gamma := \begin{cases} c|_{E_i} & \text{if } \mathbf{u} \cdot \mathbf{n}_\gamma \geq 0, \\ c|_{E_j} & \text{if } \mathbf{u} \cdot \mathbf{n}_\gamma < 0. \end{cases}$$

The usual Sobolev norm on Ω is denoted by $\|\cdot\|_{m,\Omega}$ [1]. For a positive number m, the broken Sobolev norm is defined as

$$|\!|\!| \phi |\!|\!|_m^2 := \sum_{E \in \mathcal{E}_h} \|\phi\|_{m,E}^2 . \tag{2.11}$$

The discontinuous finite element space is taken to be

$$\mathcal{D}_r(\mathcal{E}_h) := \left\{ \phi \in L^2(\Omega) : \ \phi|_E \in \mathbb{P}_r(E), \ E \in \mathcal{E}_h \right\} \tag{2.12}$$

or

$$\mathcal{D}_r(\mathcal{E}_h) := \left\{ \phi \in L^2(\Omega) : \ \phi|_E \in \mathbb{Q}_r(E), \ E \in \mathcal{E}_h \right\}, \tag{2.13}$$

where $\mathbb{P}_r(E)$ denotes the space of polynomials of total degree less than or equal to r on E, and $\mathbb{Q}_r$ is the tensor product of the polynomial spaces of degree less than or equal to r in each spatial dimension.

The inner product in $L^2(\Omega)$ or $\left(L^2(\Omega)\right)^d$ is indicated by $(\cdot,\cdot)$ and the inner product in the boundary function space $L^2(\gamma)$ is indicated by $(\cdot,\cdot)_\gamma$. The norm $\left(L^p(\Omega)\right)^d$ for a vector-valued function is defined as

$$\|\mathbf{u}\|_{(L^p(\Omega))^d} := \|(|\mathbf{u}|)\|_{L^p(\Omega)} ,$$

where $|\cdot|$ is the standard vector 2-norm defined by $|\mathbf{u}| := (\mathbf{u} \cdot \mathbf{u})^{1/2}$. For simplicity, the norms $\|\cdot\|_{L^2(\Omega)}$ and $\|\cdot\|_{(L^2(\Omega))^d}$ are also written as $\|\cdot\|_0$ for scalar-valued and vector-valued functions, respectively.

We shall use the following *hp*-approximation results, which can be proved using the techniques in [3, 4]. Let $E \in \mathcal{E}_h$, let $\phi \in H^s(E)$, and let h_E be the diameter of E. Then there exists a constant K independent of ϕ, r, and h_E and a sequence of $z_r^{h_E} \in \mathbb{P}_r(E)$, $r = 1, 2, \ldots$, such that

$$\begin{cases} \left\| \phi - z_r^{h_E} \right\|_{q,E} \leq K \frac{h_E^{\mu-q}}{r^{s-q}} \|\phi\|_{s,E} , & 0 \leq q < s, \\ \left\| \phi - z_r^{h_E} \right\|_{q,\partial E} \leq K \frac{h_E^{\mu-q-\frac{1}{2}}}{r^{s-q-\frac{1}{2}}} \|\phi\|_{s,E} , & 0 < q + \frac{1}{2} < s, \end{cases} \tag{2.14}$$

where $\mu = \min(r+1, s)$. These results apply directly to the DG space $\mathcal{D}_r(\mathcal{E}_h)$ for possibly nonconforming meshes, and they also apply to the CG space $\mathcal{D}_r(\mathcal{E}_h) \cap C(\Omega)$ for conforming meshes containing only triangles or tetrahedra when $\mathbb{P}_r$ is used.

We shall also use the following inverse estimates, which can be derived using the method in [24]. Let $E \in \mathcal{E}_h$, let $v \in \mathbb{P}_r(E)$ (or $v \in \mathbb{Q}_r(E)$), and let h_E be the diameter of E. Then there exists a constant K independent of v, r, and h_E such that

$$\begin{cases} \|D^q v\|_{0,\partial E} \le K \frac{r}{h_E^{1/2}} \|D^q v\|_{0,E}, & q \ge 0, \\ \left\|D^{q+1} v\right\|_{0,E} \le K \frac{r^2}{h_E} \|D^q v\|_{0,E}, & q \ge 0. \end{cases} \tag{2.15}$$

2.3. Discontinuous Galerkin schemes. For the flow problem, we introduce the bilinear form $a(p,\psi)$ and the linear functional $l(\psi)$ as follows:

$$\begin{aligned} a(p,\psi) := & \sum_{E\in\mathcal{E}_h} \int_E \mathbf{K}\nabla p \cdot \nabla\psi + J_\sigma(p,\psi) + J_{\mathrm{D},\sigma}(p,\psi) \\ & - \sum_{\gamma\in\Gamma_h} \int_\gamma \{\mathbf{K}\nabla p\cdot\mathbf{n}_\gamma\}[\psi] - s_{\mathrm{form}} \sum_{\gamma\in\Gamma_h} \int_\gamma \{\mathbf{K}\nabla\psi\cdot\mathbf{n}_\gamma\}[p] \\ & - \sum_{\gamma\in\Gamma_{h,\mathrm{D}}} \int_\gamma \mathbf{K}\nabla p\cdot\mathbf{n}_\gamma\psi - s_{\mathrm{form}} \sum_{\gamma\in\Gamma_{h,\mathrm{D}}} \int_\gamma \mathbf{K}\nabla\psi\cdot\mathbf{n}_\gamma p, \\ l(\psi) := & (q,\psi) + J_{\mathrm{D},\sigma}(p_B,\psi) - s_{\mathrm{form}} \sum_{\gamma\in\Gamma_{h,\mathrm{D}}} \int_\gamma \mathbf{K}\nabla\psi\cdot\mathbf{n}_\gamma p_B - \sum_{\gamma\in\Gamma_{h,\mathrm{N}}} \int_\gamma \psi u_B, \end{aligned}$$

where $s_{\mathrm{form}} = -1$ for NIPG [22] or OBB-DG [20], $s_{\mathrm{form}} = 1$ for SIPG [25, 28, 33], and $s_{\mathrm{form}} = 0$ for IIPG [14, 25, 28]. The interior and boundary penalty terms $J_\sigma(p,\psi)$ and $J_{\mathrm{D},\sigma}(p,\psi)$ are defined as

$$\begin{aligned} J_\sigma(p,\psi) &:= \sum_{\gamma\in\Gamma_h} \frac{r^2\sigma_\gamma}{h_\gamma} \int_\gamma [p][\psi], \\ J_{\mathrm{D},\sigma}(p,\psi) &:= \sum_{\gamma\in\Gamma_{h,\mathrm{D}}} \frac{r^2\sigma_\gamma}{h_\gamma} \int_\gamma p\psi, \end{aligned}$$

where the penalty parameter σ_γ is a constant on each face γ. We assume $0 < \sigma_0 \le \sigma_\gamma \le \sigma_m$ except for OBB-DG.

The DG scheme for the flow equation is to seek $P^{DG} \in \mathcal{D}_r(\mathcal{E}_h)$ satisfying

$$a\left(P^{DG}, v\right) = l(v) \qquad \forall v \in \mathcal{D}_r(\mathcal{E}_h).$$

For the transport equation, we can also employ DG to obtain a numerical solution of the concentration by seeking $C^{DG}(\cdot,t) \in \mathcal{D}_r(\mathcal{E}_h)$ such that

$$\left(\frac{\partial\phi C^{DG}}{\partial t}, w\right) + B(C^{DG}, w) = L(w) \quad \forall w \in \mathcal{D}_r(\mathcal{E}_h), \quad t \in (0,T], \tag{2.16}$$

$$\left(\phi C^{DG}, w\right) = (\phi c_0, w) \quad \forall w \in \mathcal{D}_r(\mathcal{E}_h), \quad t = 0, \tag{2.17}$$

with the bilinear form $B(c,w)$ and the linear functional $L(w)$ being defined as

$$\begin{aligned} B(c,w) := & \sum_{E\in\mathcal{E}_h} \int_E (\mathbf{D}\nabla c - c\mathbf{u})\cdot\nabla w - \int_\Omega q^- cw \\ & - \sum_{\gamma\in\Gamma_h} \int_\gamma \{\mathbf{D}\nabla c\cdot\mathbf{n}_\gamma\}[w] - s_{\mathrm{form}} \sum_{\gamma\in\Gamma_h} \int_\gamma \{\mathbf{D}\nabla w\cdot\mathbf{n}_\gamma\}[c] \end{aligned} \tag{2.18}$$

$$+\sum_{\gamma\in\Gamma_h}\int_\gamma c^*\mathbf{u}\cdot\mathbf{n}_\gamma\,[w]+\sum_{\gamma\in\Gamma_{h,\text{out}}}\int_\gamma c\mathbf{u}\cdot\mathbf{n}_\gamma w+J_\sigma\left(c,w\right),$$

$$L(w):=\int_\Omega c_w q^+ w-\sum_{\gamma\in\Gamma_{h,\text{in}}}\int_\gamma c_B\mathbf{u}\cdot\mathbf{n}_\gamma w+\int_\Omega r(c)w, \tag{2.19}$$

where q^+ is the injection source term, and q^- is the extraction source term, i.e.,

$$q^+:=\max\left(q,0\right),\quad q^-:=\min\left(q,0\right).$$

For notational convenience, we use the same symbol r to represent the degree of approximation for both the flow and the transport equations. However, different degrees of approximation can apply separately to flow and transport. Similarly, the parameter s_{form} in DG could be different for flow and transport.

We note that the DG scheme for transport coincides with the finite volume scheme or the Godunov scheme if the lowest-order approximation space (i.e., the space of piecewise constant functions) is taken for treating pure advection processes, which will be used for the transport examples in section 4.

It is known that the above DG scheme for flow and transport has a unique solution; in addition, all four primal DG versions possess optimal convergence in the energy norm, while SIPG has optimal convergence also in the L_2 norm [25, 28]. Moreover, all DG versions satisfy the elementwise mass conservation for both flow and transport. In particular, the DG approximation of the Darcy velocity satisfies on each element E the following local mass balance property for overall fluid:

$$\int_{\partial E\setminus\Gamma_{\text{N}}}\mathbf{u}^{DG}\cdot\mathbf{n}_{\partial E}ds=\int_E qdx-\int_{\partial E\cap\Gamma_{\text{N}}}u_B ds, \tag{2.20}$$

where the normal component of DG velocity is defined as

$$\mathbf{u}^{DG}\cdot\mathbf{n}_{\partial E}:=-\left\{\mathbf{K}\nabla P^{DG}\cdot\mathbf{n}_{\partial E}\right\}+\frac{r^2\sigma_\gamma}{h_\gamma}\left(P^{DG}\big|_E-P^{DG}\big|_{\Omega\setminus\overline{E}}\right),$$

with $P^{DG}\big|_{\Omega\setminus\overline{E}}$ being understood as p_B when $x\in\Gamma_{\text{D}}$.

2.4. Continuous Galerkin schemes. For the CG schemes, we use the space of continuous piecewise polynomials

$$\mathcal{D}_r^C\left(\mathcal{E}_h\right):=\mathcal{D}_r\left(\mathcal{E}_h\right)\cap C(\Omega).$$

The CG scheme for the flow equation is to seek $P^{CG}\in\mathcal{D}_r^C\left(\mathcal{E}_h\right)$ satisfying

$$a\left(P^{CG},v\right)=l(v)\qquad\forall v\in\mathcal{D}_r^C\left(\mathcal{E}_h\right).$$

Here, the boundary conditions are still enforced weakly. It has been reported that weak enforcement of boundary conditions is usually superior to the strong enforcement, which holds even for CG [7]. All the interior face terms vanish in the above CG weak formulation. In fact, the above CG weak formulation is equivalent to the following reduced form:

$$a_{CG}\left(P^{CG},v\right)=l(v)\qquad\forall v\in\mathcal{D}_r^C\left(\mathcal{E}_h\right),$$

TABLE 1
The numbers of unknowns for CG, DG, and EG on a rectangular mesh with N^d elements.

	2D domain	3D domain
Linear CG	$(N+1)^2 = N^2 + \mathcal{O}(N)$	$N^3 + \mathcal{O}(N^2)$
Linear DG	$4N^2$	$8N^3$
Linear EG	$(N+1)^2 + N^2 - 1 = 2N^2 + \mathcal{O}(N)$	$2N^3 + \mathcal{O}(N^2)$
Quadratic CG	$(2N+1)^2 = 4N^2 + \mathcal{O}(N)$	$8N^3 + \mathcal{O}(N^2)$
Quadratic DG	$9N^2$	$27N^3$
Quadratic EG	$(2N+1)^2 + N^2 - 1 = 5N^2 + \mathcal{O}(N)$	$9N^3 + \mathcal{O}(N^2)$

TABLE 2
The numbers of unknowns for CG, DG, and EG on an unstructured mesh with N_E triangles/tetrahedra, N_e edges, and N_n nodes.

	2D domain	3D domain
Linear CG	$N_n \approx \frac{1}{2} N_E$	N_n
Linear DG	$3N_E$	$4N_E$
Linear EG	$N_n + N_E \approx \frac{3}{2} N_E$	$N_n + N_E$
Quadratic CG	$N_n + N_e \approx 2N_E$	$N_n + N_e$
Quadratic DG	$6N_E$	$10N_E$
Quadratic EG	$N_n + N_e + N_E \approx 3N_E$	$N_n + N_e + N_E$

where

$$a_{CG}(p,\psi) := \sum_{E\in\mathcal{E}_h} \int_E \mathbf{K}\nabla p\cdot\nabla\psi + J_{\mathrm{D},\sigma}(p,\psi) - \sum_{\gamma\in\Gamma_{h,\mathrm{D}}} \int_\gamma \mathbf{K}\nabla p\cdot\mathbf{n}_\gamma\psi - s_{\mathrm{form}} \sum_{\gamma\in\Gamma_{h,\mathrm{D}}} \int_\gamma \mathbf{K}\nabla\psi\cdot\mathbf{n}_\gamma p.$$

We remark that some desired properties of DG are lost when approximation is restricted to continuous spaces. For example, it is hard to treat nonmatching meshes and it is difficult to combine $\mathbb{P}$ approximations with quadrilaterals in CG. Moreover, we no longer have local mass conservation with CG approximations.

2.5. Enriched Galerkin schemes. We now propose new schemes that combine the advantages of both CG and DG. In this proposed approach, the local mass conservation of DG is maintained, while the number of unknowns is close to that of CG. This is made possible by enriching the CG approximation space with piecewise constants. To be more specific, we define $\mathcal{D}_r^{C0}(\mathcal{E}_h) := \mathcal{D}_r^C(\mathcal{E}_h) \cup \mathcal{D}_0(\mathcal{E}_h)$ and seek $P^{EG} \in \mathcal{D}_r^{C0}(\mathcal{E}_h)$ satisfying

$$a\left(P^{EG}, v\right) = l(v) \qquad \forall v \in \mathcal{D}_r^{C0}(\mathcal{E}_h). \tag{2.21}$$

The number of degrees of freedom in EG is slightly larger than that of CG, but much smaller than that of DG, especially for low-order approximations. Table 1 compares the numbers of unknowns from CG, DG, and EG on a rectangular mesh, where $\mathbb{Q}$ approximations are used for all elements. The degrees of freedom in EG contain those in CG and additionally those for the piecewise constants. We note that the global constant function is already contained in the CG space; consequently, the EG scheme has $(N^d - 1)$ more degrees of freedom than CG on a d-dimensional rectangular mesh with N^d elements. Table 2 compares the numbers of unknowns from

CG, DG, and EG on an unstructured mesh containing triangles (two dimensions) or tetrahedra (three dimensions). Here N_E, N_e, and N_n denote the numbers of elements, edges, and nodes, respectively. We have assumed that $N_e \approx \frac{3}{2}N_E$ and $N_n \approx \frac{1}{2}N_E$ for the two-dimensional mesh.

The existence and uniqueness of a solution of the EG formulation can be shown using an argument similar to the one for analyzing DG [25, 28]. After the EG pressure is obtained by solving (2.21), the EG velocity $\mathbf{u}^{EG}$ is then defined below:

$$\mathbf{u}^{EG} = -\mathbf{K}\nabla P^{EG}, \quad x \in E,\ E \in \mathcal{E}_h, \tag{2.22}$$

$$\mathbf{u}^{EG}\cdot\mathbf{n} = -\left\{\mathbf{K}\nabla P^{EG}\cdot\mathbf{n}\right\} + \frac{r^2\sigma_\gamma}{h_\gamma}\left(P^{EG}\big|_{E_i} - P^{EG}\big|_{E_j}\right), \tag{2.23}$$

$$x \in \gamma = \partial\overline{E_i}\cap\partial\overline{E_j},\ E_i, E_j \in \mathcal{E}_h \text{ and } \mathbf{n} \text{ exterior to } E_i,$$

$$\mathbf{u}^{EG}\cdot\mathbf{n} = u_B, \quad x \in \Gamma_N, \tag{2.24}$$

$$\mathbf{u}^{EG}\cdot\mathbf{n} = -\mathbf{K}\nabla P^{EG}\cdot\mathbf{n} + \frac{r^2\sigma_\gamma}{h_\gamma}\left(P^{EG} - p_B\right), \quad x \in \Gamma_D. \tag{2.25}$$

Here, $\mathbf{u}^{EG}$ is defined at every interior point in each element, but only the normal velocity component $\mathbf{u}^{EG}\cdot\mathbf{n}$ is defined on element interfaces and on domain boundaries, as this is all the information we will need in our numerical schemes for transport.

A computed velocity $\mathbf{u}^h$ is said to be locally conservative if

$$\int_{\partial E}\mathbf{u}^h\cdot\mathbf{n}_{\partial E}ds = \int_E q dx.$$

Local conservation is retained in EG and DG but not in CG.

THEOREM 2.1 (local conservation of EG). *The EG velocity $\mathbf{u}^{EG}$ defined above is locally conservative.*

Proof. The local conservation of EG can be shown using a classical argument. We summarize it here for completeness. From the EG numerical scheme, we fix an element E and take the test function $v \in \mathcal{D}_r^{C0}(\mathcal{E}_h)$ with $v|_E = 1$, $v|_{\Omega\setminus E} = 0$. The resultant equation represents the elementwise conservative property. ∎

We use an operator $\mathcal{R}_q$ to compute the local conservation residual for a given velocity approximation on element faces. The operator $\mathcal{R}_q$ is a mapping from $L^1(\Gamma_h)$ onto $D_0(\mathcal{E}_h)$ defined by

$$\int_E \mathcal{R}_q(\mathbf{u}^h\cdot\mathbf{n}_{\partial E})dx = \int_E q dx - \int_{\partial E}\mathbf{u}^h\cdot\mathbf{n}_{\partial E}ds \tag{2.26}$$

for all $\mathbf{u}^h\cdot\mathbf{n}_{\partial E} \in L^1(\Gamma_h)$ and all $E \in \mathcal{E}_h$. Clearly, $\mathbf{u}^h$ is locally conservative if and only if $\mathcal{R}_q(\mathbf{u}^h\cdot\mathbf{n}_{\partial E}) = 0$. Moreover, $\mathbf{u}^h$ is globally conservative if and only if $\int_\Omega \mathcal{R}_q(\mathbf{u}^h\cdot\mathbf{n}_{\partial E}) = 0$. From the above discussion, we know $\mathcal{R}_q(\mathbf{u}^{DG}\cdot\mathbf{n}_{\partial E}) = \mathcal{R}_q(\mathbf{u}^{EG}\cdot\mathbf{n}_{\partial E}) = 0$, but $\mathcal{R}_q(\mathbf{u}^{CG}\cdot\mathbf{n}_{\partial E})$ is generally a nonzero quantity, which can be used to characterize the violation level of local conservation.

3. Analysis on the enriched Galerkin schemes. We now discuss the convergence properties of the EG schemes.

THEOREM 3.1 (error estimates on EG pressure). *Let p be the solution to* (2.1)–(2.3). *Assume that p and ∇p are essentially bounded, and that $p \in H^s(\mathcal{E}_h)$. Consider a mesh such that the hp-approximation property* (2.14) *holds for the EG finite element*

space. Let p^{EG} be the EG solution to (2.21)*. If the penalty parameters are sufficiently large, then there exists a constant C independent of h and r such that*

$$\|\mathbf{K}^{\frac{1}{2}}\nabla\left(P^{EG}-p\right)\|_0+\sqrt{J_\sigma\left(P^{EG},P^{EG}\right)}+\sqrt{J_{\mathrm{D},\sigma}\left(P^{EG}-p,P^{EG}-p\right)}\leq C\frac{h^{\mu-1}}{r^{s-3/2}},$$

where $\mu=\min(r+1,s)$, $r\geq 1$, $s\geq 2$.

Proof. Let $\widehat{p}\in\mathcal{D}_r^{C0}(\mathcal{E}_h)$ be an interpolant of the pressure p such that the *hp*-approximation property (2.14) holds. We define

$$\xi=P^{EG}-p,\quad \xi^I=p-\widehat{p},\quad \xi^A=P^{EG}-\widehat{p}=\xi+\xi^I. \tag{3.1}$$

Subtracting the weak formulation from the EG scheme equation, we have $a(\xi,v)=0$ for any $v\in\mathcal{D}_r^{C0}(\mathcal{E}_h)$. Splitting ξ as $\xi=\xi^A-\xi^I$ and choosing $v=\xi^A$, we have

$$a(\xi^A,\xi^A)=a(\xi^I,\xi^A). \tag{3.2}$$

We first consider the left-hand side of error equation (3.2):

$$\begin{aligned}
&a(\xi^A,\xi^A)\\
&=\sum_{E\in\mathcal{E}_h}\int_E\mathbf{K}\nabla\xi^A\cdot\nabla\xi^A+J_\sigma\left(\xi^A,\xi^A\right)+J_{\mathrm{D},\sigma}\left(\xi^A,\xi^A\right)\\
&\quad-(1+s_{\mathrm{form}})\sum_{\gamma\in\Gamma_h}\int_\gamma\left\{\mathbf{K}\nabla\xi^A\cdot\mathbf{n}_\gamma\right\}\left[\xi^A\right]\\
&\quad-(1+s_{\mathrm{form}})\sum_{\gamma\in\Gamma_{h,\mathrm{D}}}\int_\gamma\mathbf{K}\nabla\xi^A\cdot\mathbf{n}_\gamma\xi^A.
\end{aligned}$$

The first three terms in the above equation are nonnegative, and the fourth term can be bounded using the inverse estimates (2.15):

$$\begin{aligned}
&\left|(1+s_{\mathrm{form}})\sum_{\gamma\in\Gamma_h}\int_\gamma\left\{\mathbf{K}\nabla\xi^A\cdot\mathbf{n}_\gamma\right\}\left[\xi^A\right]\right|\\
&\leq\frac{h}{Cr^2}\sum_{E\in\mathcal{E}_h}\left\|\mathbf{K}^{\frac{1}{2}}\nabla\xi^A\cdot\mathbf{n}\right\|_{0,\partial E}^2+\frac{Cr^2}{h}\sum_{\gamma\in\Gamma_h}\left\|\left[\xi^A\right]\right\|_{0,\gamma}^2\\
&\leq\frac{1}{4}\|\mathbf{K}^{\frac{1}{2}}\nabla\xi^A\|_0^2+\frac{1}{2}J_\sigma\left(\xi^A,\xi^A\right),
\end{aligned}$$

where the two constants C could have different values, and the second constant C can be absorbed by choosing penalty parameters sufficiently large so that $\sigma_0\geq 2C$. Similarly, we can choose penalty parameters to be sufficiently large to obtain

$$\begin{aligned}
&\left|(1+s_{\mathrm{form}})\sum_{\gamma\in\Gamma_{h,\mathrm{D}}}\int_\gamma\mathbf{K}\nabla\xi^A\cdot\mathbf{n}_\gamma\xi^A\right|\\
&\leq\frac{1}{4}\|\mathbf{K}^{\frac{1}{2}}\nabla\xi^A\|_0^2+\frac{1}{2}J_{\mathrm{D},\sigma}\left(\xi^A,\xi^A\right).
\end{aligned}$$

We then infer

$$2a(\xi^A,\xi^A)\geq\|\mathbf{K}^{\frac{1}{2}}\nabla\xi^A\|_0^2+J_\sigma\left(\xi^A,\xi^A\right)+J_{\mathrm{D},\sigma}\left(\xi^A,\xi^A\right).$$

Now we bound the right-hand side of the error equation (3.2) by rewriting it as

$$\begin{aligned}
&a(\xi^I, \xi^A) \\
&= \sum_{E\in\mathcal{E}_h} \int_E \mathbf{K}\nabla\xi^I \cdot \nabla\xi^A + J_\sigma\left(\xi^I, \xi^A\right) + J_{\mathrm{D},\sigma}\left(\xi^I, \xi^A\right) \\
&\quad - \sum_{\gamma\in\Gamma_h} \int_\gamma \left\{\mathbf{K}\nabla\xi^I \cdot \mathbf{n}_\gamma\right\}\left[\xi^A\right] - s_{\mathrm{form}} \sum_{\gamma\in\Gamma_h} \int_\gamma \left\{\mathbf{K}\nabla\xi^A \cdot \mathbf{n}_\gamma\right\}\left[\xi^I\right] \\
&\quad - \sum_{\gamma\in\Gamma_{h,\mathrm{D}}} \int_\gamma \mathbf{K}\nabla\xi^I \cdot \mathbf{n}_\gamma \xi^A - s_{\mathrm{form}} \sum_{\gamma\in\Gamma_{h,\mathrm{D}}} \int_\gamma \mathbf{K}\nabla\xi^A \cdot \mathbf{n}_\gamma \xi^I \\
&=: \sum_{i=1}^{7} T_i.
\end{aligned}$$

Let ϵ be a fixed positive constant that can be chosen arbitrarily small. Term T_1 can be bounded using the Cauchy–Schwarz inequality and the approximation property:

$$\begin{aligned}
|T_1| &\le \epsilon \left\|\nabla\xi^A\right\|_0^2 + C\left\|\nabla\xi^I\right\|_0^2 \\
&\le \epsilon \left\|\nabla\xi^A\right\|_0^2 + C\frac{h^{2\mu-2}}{r^{2s-2}}.
\end{aligned}$$

Terms T_2 and T_3 can be bounded by applying the Cauchy–Schwarz inequality to the penalty term:

$$\begin{aligned}
|T_2| &\le \epsilon J_\sigma\left(\xi^A, \xi^A\right) + C J_\sigma\left(\xi^I, \xi^I\right) \\
&\le \epsilon J_\sigma\left(\xi^A, \xi^A\right) + C\frac{h^{2\mu-2}}{r^{2s-3}}, \\
|T_3| &\le \epsilon J_{\mathrm{D},\sigma}\left(\xi^A, \xi^A\right) + C\frac{h^{2\mu-2}}{r^{2s-3}}.
\end{aligned}$$

Term T_4 can be bounded similarly with the approximation property on element interfaces:

$$|T_4| \le \epsilon J_\sigma\left(\xi^A, \xi^A\right) + C\frac{h^{2\mu-2}}{r^{2s-1}}.$$

Term T_5 can be bounded using the inverse inequalities:

$$\begin{aligned}
|T_5| &\le \epsilon\frac{h}{r^2} \sum_{\gamma\in\Gamma_h} \int_\gamma \left|\left\{\nabla\xi^A \cdot \mathbf{n}_\gamma\right\}\right|^2 + C\frac{r^2}{h} \sum_{\gamma\in\Gamma_h} \int_\gamma \left|\left[\xi^I\right]\right|^2 \\
&\le \epsilon \left\|\nabla\xi^A\right\|_0^2 + C\frac{h^{2\mu-2}}{r^{2s-3}}.
\end{aligned}$$

Terms T_6 and T_7 can be bounded in a way similar to the estimation of T_4 and T_5, respectively. Substituting all these estimates into (3.2), we conclude that

$$\begin{aligned}
&\left\|\mathbf{K}^{\frac{1}{2}}\nabla\xi^A\right\|_0^2 + J_\sigma\left(\xi^A, \xi^A\right) + J_{\mathrm{D},\sigma}\left(\xi^A, \xi^A\right) \\
&\le \epsilon \left\|\nabla\xi^A\right\|_0^2 + \epsilon J_\sigma\left(\xi^A, \xi^A\right) + \epsilon J_{\mathrm{D},\sigma}\left(\xi^A, \xi^A\right) + C\frac{h^{2\mu-2}}{r^{2s-3}}.
\end{aligned}$$

The theorem then follows from the approximation properties and a triangle inequality. ∎

Remark. In Theorem 3.1, the *hp*-approximation property (2.14) has been assumed to hold for the EG finite element space. This is true for certain commonly used meshes. For example, this is certainly true for the CG finite element space with $\mathbb{P}_r$ in conforming meshes containing only triangles or tetrahedra; thus it is also true for its superspace, including the corresponding EG finite element space. Theorem 3.1 could be extended to general meshes including certain nonconforming grids, provided that we have the *hp*-approximation property (2.14). However, like CG, the EG method works better with conforming meshes with triangles or tetrahedra for convenience of implementation.

Error estimates on the EG velocity can be derived based on the above pressure estimates.

THEOREM 3.2 (error estimates on EG velocity). *Let* $\mathbf{u}$ *be the Darcy velocity solution of* (2.1)–(2.3) *and* $\mathbf{u}^{EG}$ *be the EG velocity solution as defined in* (2.22)–(2.25) *with* p^{EG} *being the EG pressure solution to* (2.21). *If all assumptions in Theorem* 3.1 *hold, then there exists a constant* C *independent of* h *and* r *such that*

$$\left\|\mathbf{u}^{EG}-\mathbf{u}\right\|_0 \le C\frac{h^{\mu-1}}{r^{s-3/2}} \tag{3.3}$$

and

$$\sum_{\gamma\in\Gamma_h\cup\Gamma_{h,D}} \left\|\mathbf{u}^{EG}\cdot\mathbf{n}_\gamma-\mathbf{u}\cdot\mathbf{n}_\gamma\right\|_{0,\gamma}^2 \le C\frac{h^{2\mu-3}}{r^{2s-5}}, \tag{3.4}$$

where $\mu=\min(r+1,s)$, $r\ge 1$, $s\ge 2$.

Proof. The estimate (3.3) follows from Theorem 3.1 and the definition of the EG velocity $\mathbf{u}^{EG}=-\mathbf{K}\nabla P^{EG}$ within element interiors (at $x\in E$, $E\in\mathcal{E}_h$), together with the assumption on the boundedness of the conductivity $\mathbf{K}$. To bound $\sum_{\gamma\in\Gamma_h}\left\|\mathbf{u}^{EG}\cdot\mathbf{n}_\gamma-\mathbf{u}\cdot\mathbf{n}_\gamma\right\|_{0,\gamma}^2$, we first let $\widehat{P}\in\mathcal{D}_r^{C0}(\mathcal{E}_h)$ be an interpolant of p such that the *hp*-result (2.14) holds. We then define $\widehat{\mathbf{u}}=-\mathbf{K}\nabla\widehat{P}$ within each element. On the element interface $\gamma=\overline{E_i}\cap\overline{E_j}$, $\widehat{\mathbf{u}}$ is defined as

$$\widehat{\mathbf{u}}|_\gamma=\{\widehat{\mathbf{u}}\}=\frac{\widehat{\mathbf{u}}|_{E_i}+\widehat{\mathbf{u}}|_{E_j}}{2}.$$

Applying the inverse estimates to the error of $\mathbf{u}^{DG}$, we have

$$\begin{aligned}
&\sum_{\gamma\in\Gamma_h}\left\|\mathbf{u}^{EG}\cdot\mathbf{n}_\gamma-\mathbf{u}\cdot\mathbf{n}_\gamma\right\|_{0,\gamma}^2\\
&\le 2\sum_{\gamma\in\Gamma_h}\left\|\mathbf{u}^{EG}\cdot\mathbf{n}_\gamma-\widehat{\mathbf{u}}\cdot\mathbf{n}_\gamma\right\|_{0,\gamma}^2+2\sum_{\gamma\in\Gamma_h}\left\|\widehat{\mathbf{u}}\cdot\mathbf{n}_\gamma-\mathbf{u}\cdot\mathbf{n}_\gamma\right\|_{0,\gamma}^2\\
&\le 2\sum_{\gamma\in\Gamma_h}\left\|\mathbf{u}^{EG}\cdot\mathbf{n}_\gamma-\widehat{\mathbf{u}}\cdot\mathbf{n}_\gamma\right\|_{0,\gamma}^2+C\frac{h^{2\mu-3}}{r^{2s-3}}\\
&= 2\sum_{\gamma\in\Gamma_h}\left\|-\left\{\mathbf{K}\nabla P^{EG}\cdot\mathbf{n}_\gamma\right\}+\frac{r^2\sigma_\gamma}{h_\gamma}\left[P^{EG}\right]-\widehat{\mathbf{u}}\cdot\mathbf{n}_\gamma\right\|_{0,\gamma}^2+C\frac{h^{2\mu-3}}{r^{2s-3}}\\
&\le 2\sum_{E_i\cup E_j=\gamma\in\Gamma_h}\left(\left\|\mathbf{u}^{EG}|_{E_i}-\widehat{\mathbf{u}}|_{E_i}\right\|_{0,\gamma}^2+\left\|\mathbf{u}^{EG}|_{E_j}-\widehat{\mathbf{u}}|_{E_j}\right\|_{0,\gamma}^2\right)
\end{aligned}$$

$$
\begin{aligned}
&+4\sum_{\gamma\in\Gamma_h}\left\|\frac{r^2\sigma_\gamma}{h_\gamma}\left[P^{EG}\right]\right\|_{0,\gamma}^2+C\frac{h^{2\mu-3}}{r^{2s-3}}\\
&\le C\frac{r^2}{h}\sum_{E\in\mathcal{E}_h}\int_E\left|\mathbf{u}^{EG}-\widehat{\mathbf{u}}\right|^2+C\frac{r^2}{h}J_\sigma\left(P^{EG},P^{EG}\right)+C\frac{h^{2\mu-3}}{r^{2s-3}}\\
&\le C\frac{r^2}{h}\sum_{E\in\mathcal{E}_h}\int_E\left|\mathbf{u}^{EG}-\mathbf{u}\right|^2+C\frac{r^2}{h}\sum_{E\in\mathcal{E}_h}\int_E\left|\mathbf{u}-\widehat{\mathbf{u}}\right|^2\\
&\quad+C\frac{r^2}{h}J_\sigma\left(P^{EG},P^{EG}\right)+C\frac{h^{2\mu-3}}{r^{2s-3}}\\
&\le C\frac{r^2}{h}\sum_{E\in\mathcal{E}_h}\int_E\left|\mathbf{u}^{EG}-\mathbf{u}\right|^2+C\frac{r^2}{h}\frac{h^{2\mu-2}}{r^{2s-2}}+C\frac{r^2}{h}J_\sigma\left(P^{EG},P^{EG}\right)+C\frac{h^{2\mu-3}}{r^{2s-3}}\\
&\le C\frac{r^2}{h}\sum_{E\in\mathcal{E}_h}\int_E\left|\mathbf{u}^{EG}-\mathbf{u}\right|^2+C\frac{r^2}{h}J_\sigma\left(P^{EG},P^{EG}\right)+C\frac{h^{2\mu-3}}{r^{2s-4}}.
\end{aligned}
$$

Substituting (3.3) and the estimate of $J_\sigma\left(P^{EG},P^{EG}\right)$ from Theorem 3.1 into the above inequality, we conclude that

$$
\sum_{\gamma\in\Gamma_h}\left\|\mathbf{u}^{EG}\cdot\mathbf{n}_\gamma-\mathbf{u}\cdot\mathbf{n}_\gamma\right\|_{0,\gamma}^2\le C\frac{h^{2\mu-3}}{r^{2s-5}}.
$$

Similar arguments together with the estimate of $J_{D,\sigma}\left(P^{EG}-p,P^{EG}-p\right)$ from Theorem 3.1 yield

$$
\sum_{\gamma\in\Gamma_{h,D}}\left\|\mathbf{u}^{EG}\cdot\mathbf{n}_\gamma-\mathbf{u}\cdot\mathbf{n}_\gamma\right\|_{0,\gamma}^2\le C\frac{h^{2\mu-3}}{r^{2s-5}}. \qquad \square
$$

4. Numerical examples. In this section, we present three numerical examples to demonstrate the strong potential of the EG method through comparison with the CG and DG methods. For each example, we solve a coupled problem of flow and transport. The flow equation is solved by CG, DG, and EG, respectively. As of the CG numerical flux on an interior face, we use the average of the directly evaluated CG fluxes on both sides of the face. The directly computed CG fluxes are used in the interior of the elements or on boundary faces. For $r=1$ (linear), NIPG is used with penalty parameter $\sigma=1$. For $r=2$ (quadratic), OBB is used and no penalty parameter is needed. The transport equation (with only advection) is solved by Godunov's scheme (or DG with a piecewise constant approximation) together with the forward Euler method of a uniform time step. The inflow boundary condition for the transport problem is $c_B=1$, and the initial concentration is zero. For each example, the same spatial mesh is used for both the flow and the transport equations. For Examples I and II, in order to display the velocity in the low permeable region(s), the velocity field is plotted with a constant magnitude and only the direction of the numerical solution is used.

4.1. Example I: An example with a poorly permeable region. In Example I, the domain is $\Omega=(0,1)^2$ containing a central subdomain $\Omega_c=(\frac{3}{8},\frac{5}{8})\times(\frac{1}{4},\frac{3}{4})$. The conductivity is a diagonal tensor $\mathbf{K}=\mathrm{diag}(K)$ with its entry K being 10^{-3} in Ω_c and 1 elsewhere, as illustrated in the top left plot of Figure 1. The boundary conditions for the flow equation are

$$
p=1,\ \text{left};\qquad p=0,\ \text{right};\qquad \mathbf{u}\cdot\mathbf{n}=0,\ \text{elsewhere}.
$$

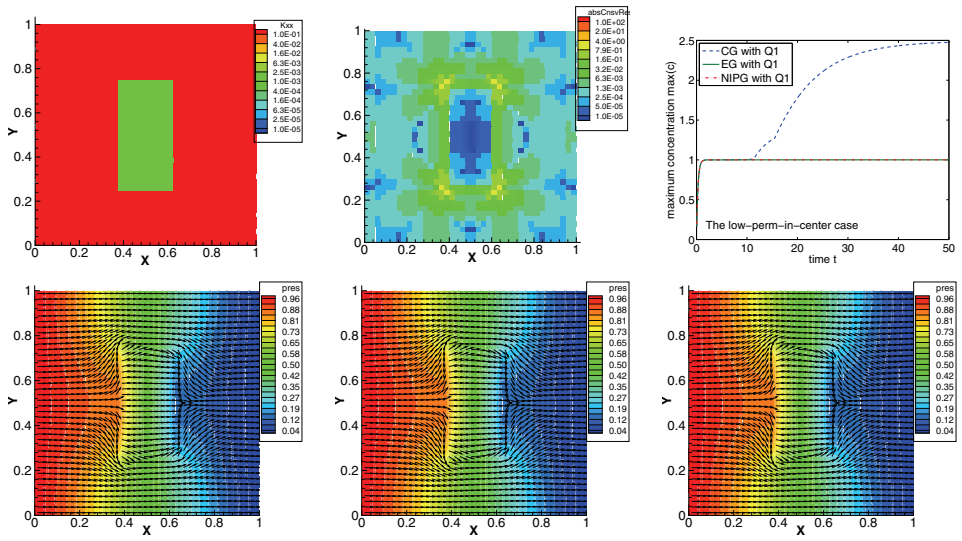

FIG. 1. *Example* I: *Simulations with linear CG, DG, and EG. Top left: conductivity; top middle: local conservation residual of the CG velocity; top right: maximum concentrations from CG, DG, and EG; bottom left: CG pressure and velocity; bottom middle: NIPG pressure and velocity; bottom right: EG pressure and velocity.*

The simulations are run using a uniform 40×40 rectangular mesh with $r = 1$ and $r = 2$. The final time in the transport problem is $T_f = 50$, and the employed uniform time step size is $\Delta t = 0.05$. The simulation results are displayed in Figures 1–4.

4.2. Example II: Random conductivity. There are actually two parts in Example II: In both parts, the domain is $\Omega = (0, 1)^2$. In Example II-A (**Rand10x10**), the diagonal entry of the conductivity $\mathbf{K} = \text{diag}(K)$ is a piecewise constant defined on a uniform 10×10 rectangular mesh; K_E (the value of K on element E) was randomly generated by a log-normal distribution with a mean of 0 and a standard deviation of 1 for $\log(K_E)$; this conductivity is illustrated in the left plot of Figure 5. In Example II-B (**Rand40x40**), the conductivity $\mathbf{K} = \text{diag}(K)$ is generated with almost the same approach as that in Example II-A except that it is now defined on a uniform 40×40 rectangular mesh; thus it has stronger heterogeneity than the conductivity in Example II-A. Figure 7 includes a plot of $\mathbf{K}$ in Example II-B. For both part A and part B, the boundary conditions for the flow equation are still

$$p = 1, \quad \text{left}; \qquad p = 0, \quad \text{right}; \qquad \mathbf{u} \cdot \mathbf{n} = 0, \quad \text{elsewhere}.$$

The spatial mesh for the EG discretization is a uniform 40×40 rectangular mesh for both parts. Linear approximations ($r = 1$) are employed for the flow equation; $T_f = 1$ and $\Delta t = 0.0002$ are adopted for the transport equation. The simulation results are summarized in Figures 5–9.

It is worthy to note that the concentration overshoots exhibited by the CG solutions in **Rand40x40** are worse than those in **Rand10x10** as seen in Figure 9. This shows that increased heterogeneity in permeability or conductivity deteriorates concentration simulations when nonconservative velocities are used.

4.3. Example III: A domain with a circular hole. In this example, the domain is $\Omega = (0, 1)^2 \setminus \Omega_c$, where Ω_c is a disk with center at (0.5, 0.5) and radius 0.2.

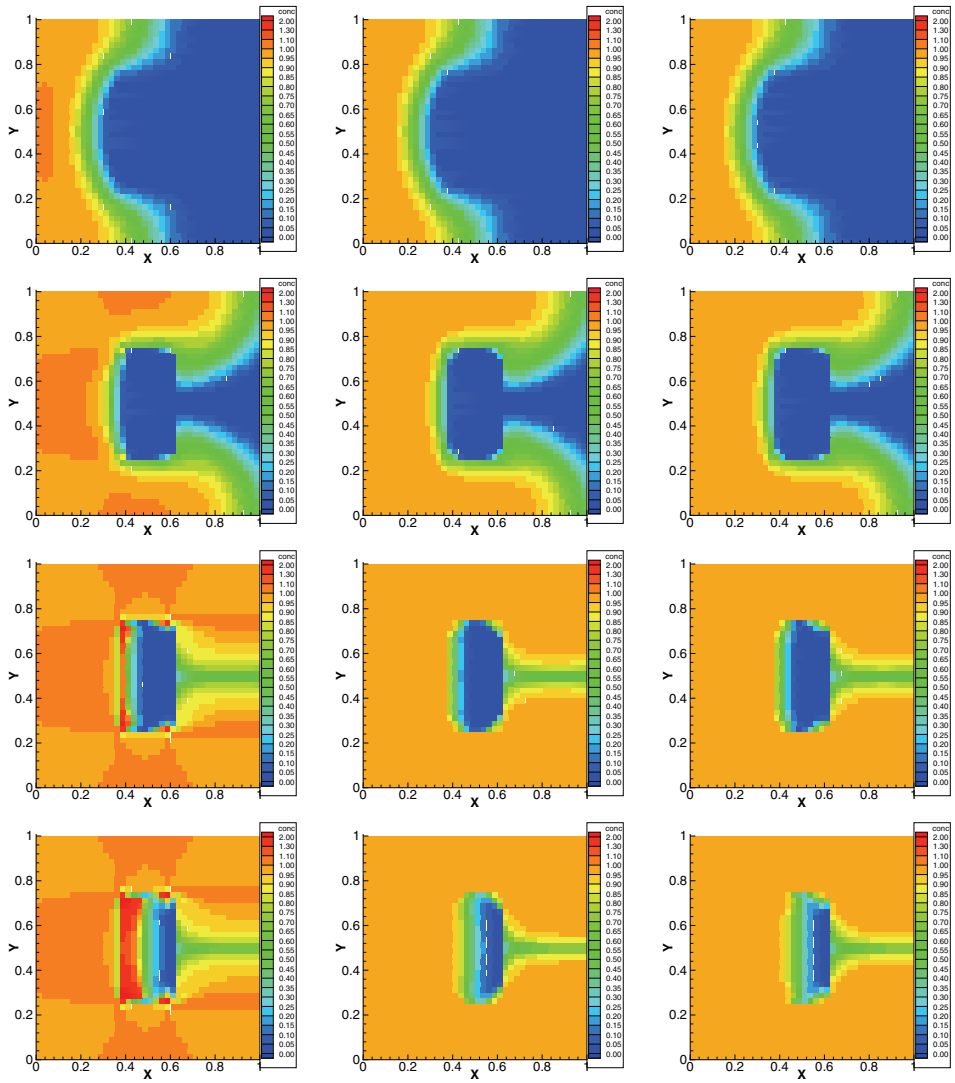

FIG. 2. *Example* I: *Concentration simulations with linear CG, DG, and EG. Left column: linear CG; middle column: linear NIPG; right column: linear EG; rows* 1 *through* 4: *time* $t = 5$, 10, 25, *and* 50.

The conductivity is the 2×2 identity matrix. A triangular mesh is generated using the PDE toolbox in MATLAB. Again, the boundary conditions for the flow problem are

$$p = 1, \quad \text{left}; \qquad p = 0, \quad \text{right}; \qquad \mathbf{u} \cdot \mathbf{n} = 0, \quad \text{elsewhere}.$$

Note that now "elsewhere" also includes the inner circular boundary. Linear elements ($r = 1$) are used with the EG approximation for flow. For the transport problem, we have $T_f = 2$ and $\Delta t = 0.002$. The simulation results are displayed in Figures 10–11.

With the above three examples, we have the following observations:

(i) Concentration overshoots from using a CG velocity are small early on, but

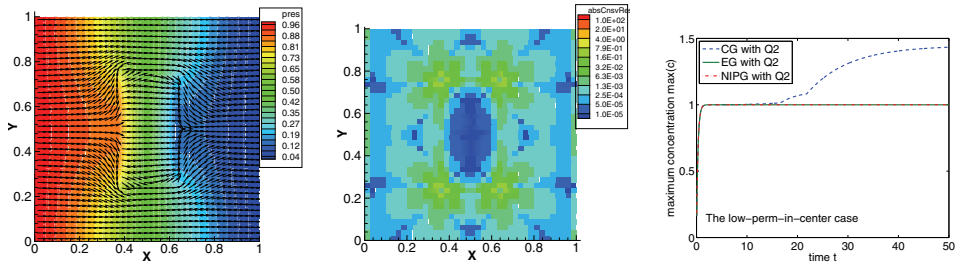

FIG. 3. *Example* I: *Simulations with quadratic CG, DG, and EG. Left: CG pressure and velocity; middle: local conservation residual of the CG velocity; right: maximum concentrations from CG, DG, and EG.*

the overshoots increase significantly as time goes on, due to the accumulation effect. Clearly, concentration overshoots are always a problem for long-time simulations if a CG velocity is used.

(ii) Maximal concentrations obtained from using a CG velocity tend to go to a limit (i.e., do not blow up to infinity). When the concentration increases to a level sufficiently high for a particular element, the extra outflow mass due to the concentration overshoot will ultimately balance the artificial source term induced by the nonconservative velocity. For the same reason, concentration is nonnegative in the above examples.

(iii) The patterns/regions of concentration overshoots are different for the linear and the quadratic approximations. The local mass-conservation residuals from quadratic CG are usually smaller than those from linear CG on the same mesh, because improved accuracy of solutions leads to improved local mass conservation. Consequently, the concentration overshoots from using a quadratic CG velocity are also smaller than those from using a linear CG velocity. Nevertheless, the nonzero local mass-conservation residuals always cause undesired significant concentration overshoots for both linear and quadratic cases.

(iv) The concentration overshoots in the examples of random conductivities are significantly larger than the other two examples. The heterogeneity in real life geological porous media is both stronger in magnitude and wider in spanned scales than the examples given here. Consequently, we expect the local mass conservation to be even more important for real life applications.

5. Discussion and conclusions. It has been shown in this paper that by enriching CG with the lowest-order discontinuous space, our proposed EG method is equipped with local mass conservation, while its number of degrees of freedom is substantially less than that of DG, a popular method for retaining local conservation. We would like to point out that it is not necessary to enrich globally every element for constructing EG spaces; instead, we may enrich only those elements in the subregions that desire local conservation. In other words, one can add piecewise constants only to the elements where local mass conservation is needed. For example, contaminant transport might have a significant part of the domain with nearly zero concentration, where mass conservation is not that important; in this scenario, we need to enrich only the small region where the concentration of contaminants is considerable. Moreover, it is also possible to perform the enrichment adaptively after a guess solution of

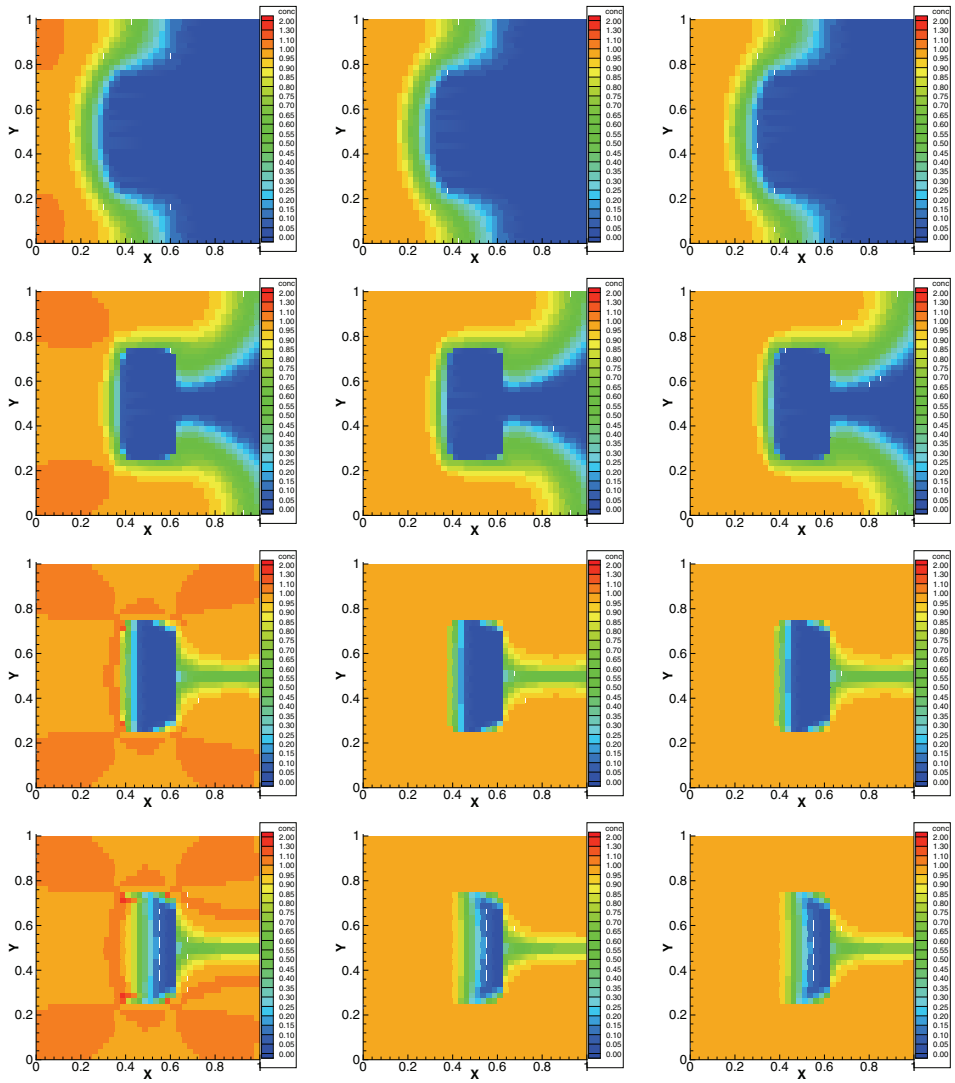

FIG. 4. *Example* I: *Concentration simulations with quadratic CG, DG, and EG. Left column: CG; middle column: OBB; right column: EG; rows* 1 *through* 4: *time* $t = 5$, 10, 25, *and* 50.

concentration is obtained.

Sometimes it is desirable to have simultaneously a continuous pressure and a locally conservative velocity (with continuous normal components). This is difficult to achieve in either CG or DG. Unlike DG, the EG method can generate a continuous pressure by using the simple continuity-recovery postprocessing of de-enrichment. That is, to get a continuous EG pressure, we simply remove the components of piecewise constant functions from the original EG pressure solution. We note that this constant function contribution to the pressure solution should be in a tiny amount anyway, since the jumps converge to zero. In addition, we note that piecewise constants do not contribute towards the calculation of the EG velocity within element interiors (although affecting the EG velocity defined on element boundaries); thus

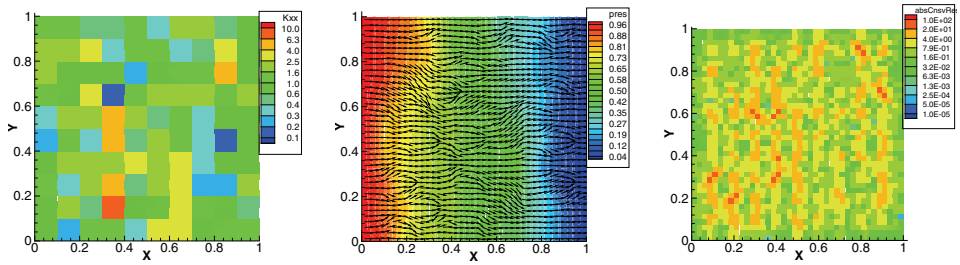

FIG. 5. *Example* II-*A: Simulations with linear CG. Left: conductivity; middle: CG pressure and velocity; right: local conservation residual of the CG velocity.*

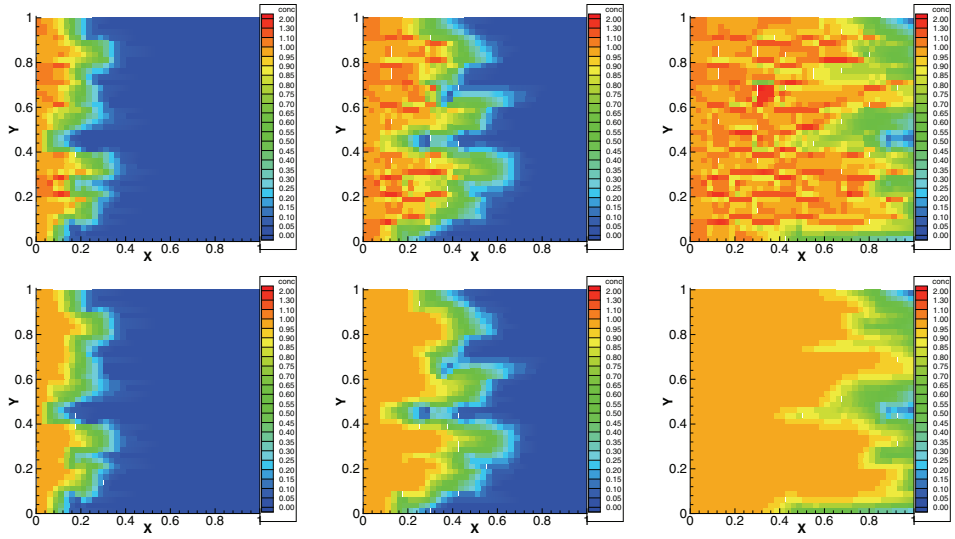

FIG. 6. *Example* II-*A: Concentration simulations with linear CG and EG. Top row: linear CG; bottom row: linear EG; columns* 1 *through* 3: *time* $t = 0.2$, 0.4, *and* 1.

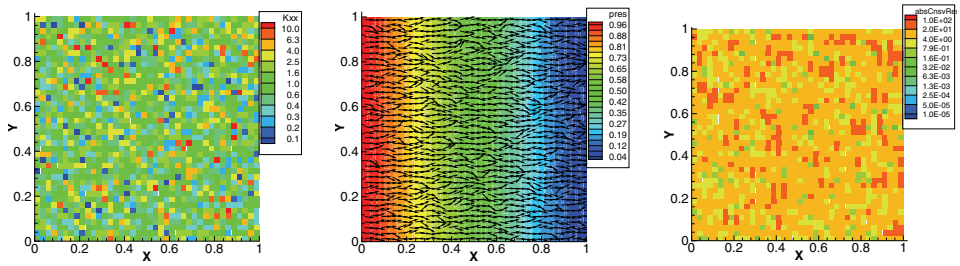

FIG. 7. *Example* II-*B: Simulations with linear CG. Left: conductivity; middle: CG pressure and velocity; right: local conservation residual of the CG velocity.*

we still have a pair of continuous pressure and locally conservative velocity that are consistent with each other at least within element interiors.

Compared with DG, the proposed EG method has the following features:

- The computational cost of EG is lower than that of DG.

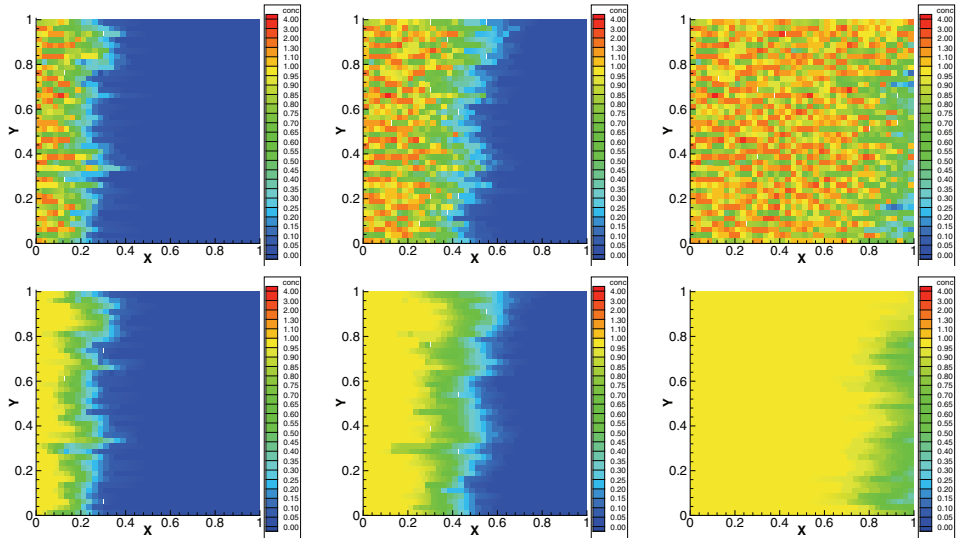

FIG. 8. *Example* II-*B: Concentration simulations with linear CG and EG. Top row: linear CG; bottom row: linear EG; columns* 1 *through* 3: *time* $t = 0.2$, 0.4, *and* 1.

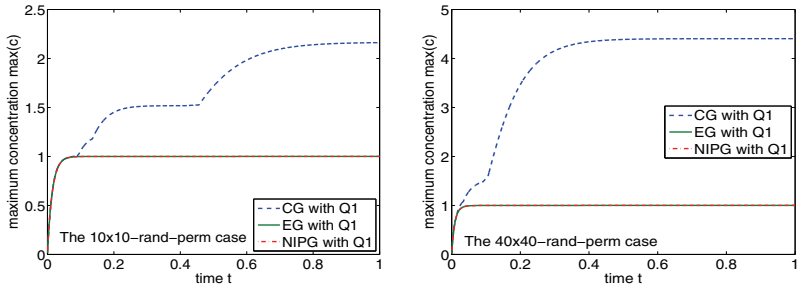

FIG. 9. *Examples* II-*A and* II-*B: Maximum concentrations of linear CG, DG, and EG solutions to Example* II-*A of random conductivity on a* 10×10 *mesh (left) and Example* II-*B of random conductivity on a* 40×40 *mesh (right).*

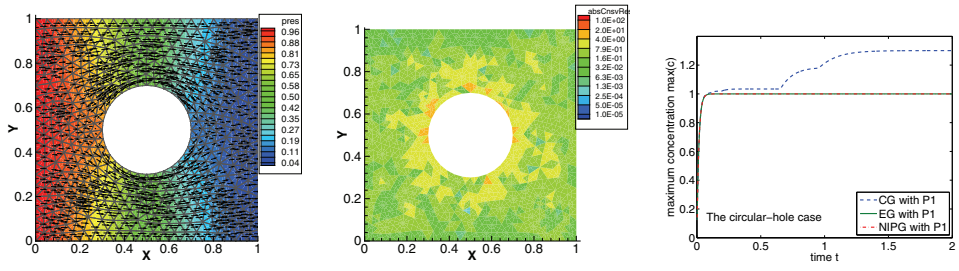

FIG. 10. *Example* III: *Simulations on a triangular mesh with linear CG, DG, and EG. Left: CG pressure and velocity; middle: local conservation residual of the CG velocity; right: maximum concentrations from linear CG, DG, and EG.*

- The implementation of EG is simpler than that of DG and is potentially more efficient, since the jumps are just constants rather than full-degree polynomi-

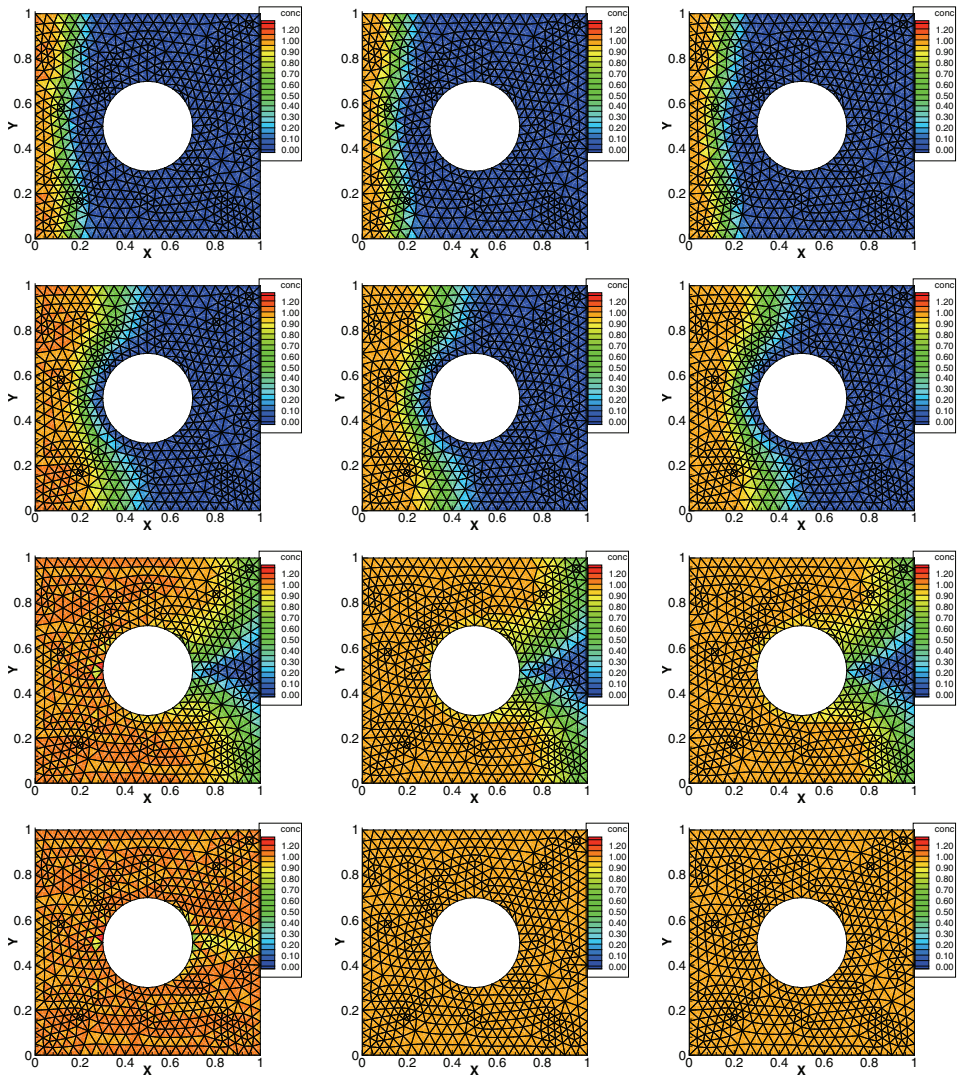

FIG. 11. *Example* III: *Concentration simulations with linear CG, DG, and EG. Left column: linear CG; middle column: linear NIPG; right column: linear EG; rows* 1 *through* 4: *time* $t = 0.2$, 0.4, 1, *and* 2.

als in DG.

- Similar to DG, a linear EG needs penalty terms, while a quadratic EG does not for antisymmetric formulations.
- EG can treat nonconforming meshes, though it is not as convenient as DG for this.
- EG is a desired method for flow when streamlines are to be constructed or when flow is coupled with transport and/or reactions.
- For very high order elements, DG is more attractive than EG.

Porous media flow involves strong heterogeneity, which makes local mass conservation indispensable to numerical simulations of flow and transport. On the other

hand, the high roughness of the solutions to these applications implies that a low-order approximation is more suitable than high orders. Both suggest that EG is a desirable method.

The theoretical analysis and numerical experiments presented in this paper have demonstrated various features of EG, especially its efficiency and accuracy, as well as its preservation of local mass conservation, as applied to single-phase porous media flow and single-species transport. Systems of multiple species with kinetic reactions can be treated similarly. Extension of EG to two-phase flow problems is our current investigation.

Acknowledgments. The authors would like to express their sincere thanks to the referees for their very valuable comments and suggestions, which have greatly improved the quality of this paper.

REFERENCES

[1] R. A. Adams and J. J. F. Fournier, *Sobolev Spaces*, 2nd ed., Academic Press, New York, 2003.

[2] D. N. Arnold, *An interior penalty finite element method with discontinuous elements*, SIAM J. Numer. Anal., 19 (1982), pp. 742–760.

[3] I. Babuška and M. Suri, *The optimal convergence rate of the p-version of the finite element method*, SIAM J. Numer. Anal., 24 (1987), pp. 750–776.

[4] I. Babuška and M. Suri, *The h-p version of the finite element method with quasi-uniform meshes*, RAIRO Modél. Math Anal. Numer., 21 (1987), pp. 199–238.

[5] I. Babuška and M. Zlámal, *Nonconforming elements in the finite element method with penalty*, SIAM J. Numer. Anal., 10 (1973), pp. 863–875.

[6] C. E. Baumann and J. T. Oden, *A discontinuous hp finite element method for convection-diffusion problems*, Comput. Methods Appl. Mech. Engrg., 175 (1999), pp. 311–341.

[7] Y. Bazilevs and T. J. R. Hughes, *Weak imposition of Dirichlet boundary conditions in fluid mechanics*, Comput. & Fluids, 36 (2007), pp. 12–26.

[8] R. Becker, E. Burman, P. Hansbo, and M. G. Larson, *A Reduced P^1-Discontinuous Galerkin Method*, Chalmers Finite Element Center Preprint 2003-13, Chalmers University of Technology, Göteborg, Sweden, 2003.

[9] Z. Chen and H. Chen, *Pointwise error estimates of discontinuous Galerkin methods with penalty for second-order elliptic problems*, SIAM J. Numer. Anal., 42 (2004), pp. 1146–1166.

[10] S. Chippada, C. N. Dawson, M. L. Martinez, and M. F. Wheeler, *A projection method for constructing a mass conservative velocity field*, Comput. Methods Appl. Mech. Engrg., 157 (1998), pp. 1–10.

[11] B. Cockburn, J. Gopalakrishnan, and H. Wang, *Locally conservative fluxes for the continuous Galerkin method*, SIAM J. Numer. Anal., 45 (2007), pp. 1742–1776.

[12] B. Cockburn, G. E. Karniadakis, and C.-W. Shu, *The development of the discontinuous Galerkin methods*, in Discontinuous Galerkin Methods, Lect. Notes Comput. Sci. Eng. 11, Springer-Verlag, Berlin, 2000, pp. 3–50.

[13] B. Cockburn and C.-W. Shu, *The local discontinuous Galerkin method for time-dependent convection-diffusion systems*, SIAM J. Numer. Anal., 35 (1998), pp. 2440–2463.

[14] C. Dawson, S. Sun, and M. F. Wheeler, *Compatible algorithms for coupled flow and transport*, Comput. Methods Appl. Mech. Engrg., 193 (2004), pp. 2565–2580.

[15] J. Douglas and T. Dupont, *Interior penalty procedures for elliptic and parabolic Galerkin methods*, in Computing Methods in Applied Sciences, Lecture Notes in Phys. 58, Springer-Verlag, Berlin, 1976, pp. 207–216.

[16] T. Hughes, G. Engel, L. Mazzei, and M. Larson, *The continuous Galerkin method is locally conservative*, J. Comput. Phys., 163 (2000), pp. 467–488.

[17] O. A. Karakashian and F. Pascal, *A posteriori error estimates for a discontinuous Galerkin approximation of second-order elliptic problems*, SIAM J. Numer. Anal., 41 (2003), pp. 2374–2399.

[18] M. G. Larson and A. J. Niklasson, *Analysis of a nonsymmetric discontinuous Galerkin method for elliptic problems: Stability and energy error estimates*, SIAM J. Numer. Anal., 42 (2004), pp. 252–264.

[19] M. G. Larson and A. J. Niklasson, *A conservative flux for the continuous Galerkin method based on discontinuous enrichment*, Calcolo, 41 (2004), pp. 65–76.
[20] J. T. Oden, I. Babuška, and C. E. Baumann, *A discontinuous hp finite element method for diffusion problems*, J. Comput. Phys., 146 (1998), pp. 491–516.
[21] J. T. Oden and L. C. Wellford, Jr., *Discontinuous finite element approximations for the analysis of shock waves in nonlinearly elastic materials*, J. Comput. Phys., 19 (1975), pp. 179–210.
[22] B. Rivière, M. F. Wheeler, and V. Girault, *A priori error estimates for finite element methods based on discontinuous approximation spaces for elliptic problems*, SIAM J. Numer. Anal., 39 (2001), pp. 902–931.
[23] D. Schötzau and C. Schwab, *Time discretization of parabolic problems by the hp-version of the discontinuous Galerkin finite element method*, SIAM J. Numer. Anal., 38 (2000), pp. 837–875.
[24] C. Schwab, *p- and hp-Finite Element Methods: Theory and Applications in Solid and Fluid Mechanics*, Oxford University Press, New York, 1998.
[25] S. Sun, *Discontinuous Galerkin Methods for Reactive Transport in Porous Media*, Ph.D. thesis, The University of Texas at Austin, Austin, TX, 2003.
[26] S. Sun and M. F. Wheeler, *Discontinuous Galerkin methods for coupled flow and reactive transport problems*, Appl. Numer. Math., 52 (2005), pp. 273–298.
[27] S. Sun and M. F. Wheeler, *$L^2(H^1)$ norm a posteriori error estimation for discontinuous Galerkin approximations of reactive transport problems*, J. Sci. Comput., 22 (2005), pp. 501–530.
[28] S. Sun and M. F. Wheeler, *Symmetric and nonsymmetric discontinuous Galerkin methods for reactive transport in porous media*, SIAM J. Numer. Anal., 43 (2005), pp. 195–219.
[29] S. Sun and M. F. Wheeler, *Anisotropic and dynamic mesh adaptation for discontinuous Galerkin methods applied to reactive transport*, Comput. Methods Appl. Mech. Engrg., 195 (2006), pp. 3382–3405.
[30] S. Sun and M. F. Wheeler, *Projections of velocity data for the compatibility with transport*, Comput. Methods Appl. Mech. Engrg., 195 (2006), pp. 653–673.
[31] S. Sun and M. F. Wheeler, *A posteriori error estimation and dynamic adaptivity for symmetric discontinuous Galerkin approximations of reactive transport problems*, Comput. Methods Appl. Mech. Engrg., 195 (2006), pp. 632–652.
[32] S. Sun and M. F. Wheeler, *Discontinuous Galerkin methods for simulating bioreactive transport of viruses in porous media*, Adv. in Water Res., 30 (2007), pp. 1696–1710.
[33] M. F. Wheeler, *An elliptic collocation-finite element method with interior penalties*, SIAM J. Numer. Anal., 15 (1978), pp. 152–161.